ORIGINAL RESEARCH ARTICLE

Deterministic Parameter Variation Versus Random-Field Reliability Assessment in Soil-Nailed Slope Stability

Aduot Madit Anhiem

Department of Civil Engineering, Universiti Teknologi PETRONAS

Supervisor: Assoc. Prof. Dr. Indra Sati Hamonangan Harahap

KEYWORDS

Reliability Based Design · Random Fields · FORM · Monte Carlo Simulation · ARBIS · Slope Stability · Soil Nailing · Probability of Failure · Factor of Safety

ARTICLE INFO

Received: September 2026

Institution: Universiti Teknologi PETRONAS

Programme: B.Eng. (Hons) Civil Engineering

ABSTRACT

Geotechnical reliability analysis of slopes traditionally relies on deterministic parameter variation using the First Order Reliability Method (FORM), which treats soil cohesion and friction angle as fixed, bounded scalars. This paper contrasts that conventional approach (Case 1) with a spatially resolved Monte Carlo Simulation (MCS) and Adaptive Radial Based Importance Sampling (ARBIS) framework grounded in random field theory (Case 2), applied to a soil-nailed slope. Results demonstrate that while FORM with set-varied parameters yields smooth, monotonically improving factors of safety as soil strength increases, random field realizations reveal non-negligible probabilities of failure even when the mean factor of safety exceeds unity a phenomenon attributable to localised weak zones created by spatial variability of cohesion and friction angle. Anchoring consistently improves the minimum factor of safety in both approaches. The random field framework better captures the physical heterogeneity of soil, supports identification of critical non-linear failure surfaces, and provides a more economically calibrated reliability-based design.

1. Introduction

Geotechnical engineering is inherently probabilistic. Soil is heterogeneous, depositional histories vary spatially, and the strength parameters most critical to slope stability cohesion (c') and friction angle (φ') fluctuate continuously throughout a soil mass. Despite this, the mainstream approach to reliability-based design (RBD) in geotechnical practice has long relied on deterministic reduction: soil properties are assigned representative scalar values that are then systematically varied across a plausible range, and the First Order Reliability Method (FORM) is applied to derive a reliability index and probability of failure.

The weakness of this "set-varied" paradigm is well-documented. Vanmarcke (1983), Baecher and Christian (2003), and Griffiths and Fenton (2009) have each demonstrated that ignoring the spatial correlation structure of soil properties leads to systematic overestimation of reliability when localised weak zones are present. When a critical failure surface passes predominantly through below-mean-strength soil, the global mean factor of safety (FOS) may remain greater than unity while the actual probability of failure is non-negligible.

This paper directly compares the two approaches denoted **Case 1** (FORM with set-varied parameters) and **Case 2** (Monte Carlo Simulation with Adaptive Radial Based Importance Sampling applied to Gaussian random field realisations) for a reinforced slope stabilised by soil nailing. The objectives are to quantify the differences in computed FOS, reliability index (β), and probability of failure (Pf); to characterise the failure modes each approach identifies; and to argue for the adoption of random field methods as the default framework for geotechnical RBD.

1.1 Why Set-Varied Parameters Can Misrepresent Field Conditions

When cohesion and friction angle are represented by single scalars even if those scalars are drawn from a statistical distribution via FORM the implicit assumption is that the soil is perfectly homogeneous within each analysis increment. Every slice of the failure surface "sees" the same strength. Real soils do not behave this way. A soft inclusion, a poorly cemented lens, or a zone of elevated pore-water content can dramatically reduce the resistance along a critical segment of the slip surface without altering the global mean. Such localised anomalies are invisible to FORM unless explicitly modelled.

Additionally, FORM linearises the performance function at the design point (the most probable failure combination of parameters). For highly non-linear failure surfaces common in heterogeneous soil profiles this linearisation introduces bias. Duncan (2000) noted that applying the same factor of safety to conditions with widely varying degrees of uncertainty is logically inconsistent. Random field theory resolves this by replacing the scalar soil model with a spatially correlated field of values, each consistent with measured variance and autocorrelation structure.

2. Model Description

2.1 Slope Geometry and Soil Nailing Configuration

The analysis domain is a two-tier slope with geometric parameters summarised below. The slope height is composed of two sections: a primary face of height **H_1 = 9.5 m** and a secondary berm of height **H_2 = 2.0 m**; the corresponding horizontal extents are W_1 = 2.546 m and W_2 = 6.0 m. Soil unit weight is γ = 18 kN/m³.

Six soil nails are installed at inclination η = 15° from horizontal, located at depths 1.0, 2.5, 4.0, 5.5, 7.0, and 8.5 m from the crest. Each nail has length L = 7.7 m, diameter d = 25 mm, yield strength Fy = 412,000 kPa, and is grouted in a drill hole of diameter 100 mm with a maximum grout–soil shear resistance of Tmax = 25 kPa. Nails are spaced Sv = 1.5 m vertically and Sh = 1.1 m horizontally. The facing panel resists a maximum normal force of TF = 10 MN.

Soil nailing is an in situ reinforcement technique that enhances slope stability by inserting passive metallic inclusions (nails) into the earth. The nails mobilise tensile resistance as the soil mass attempts to deform, redistributing forces within the system. The failure mode of a soil-nailed system is ductile: failure is gradual, providing warning before collapse a property that makes soil nailing particularly suitable for occupied or trafficked slopes.

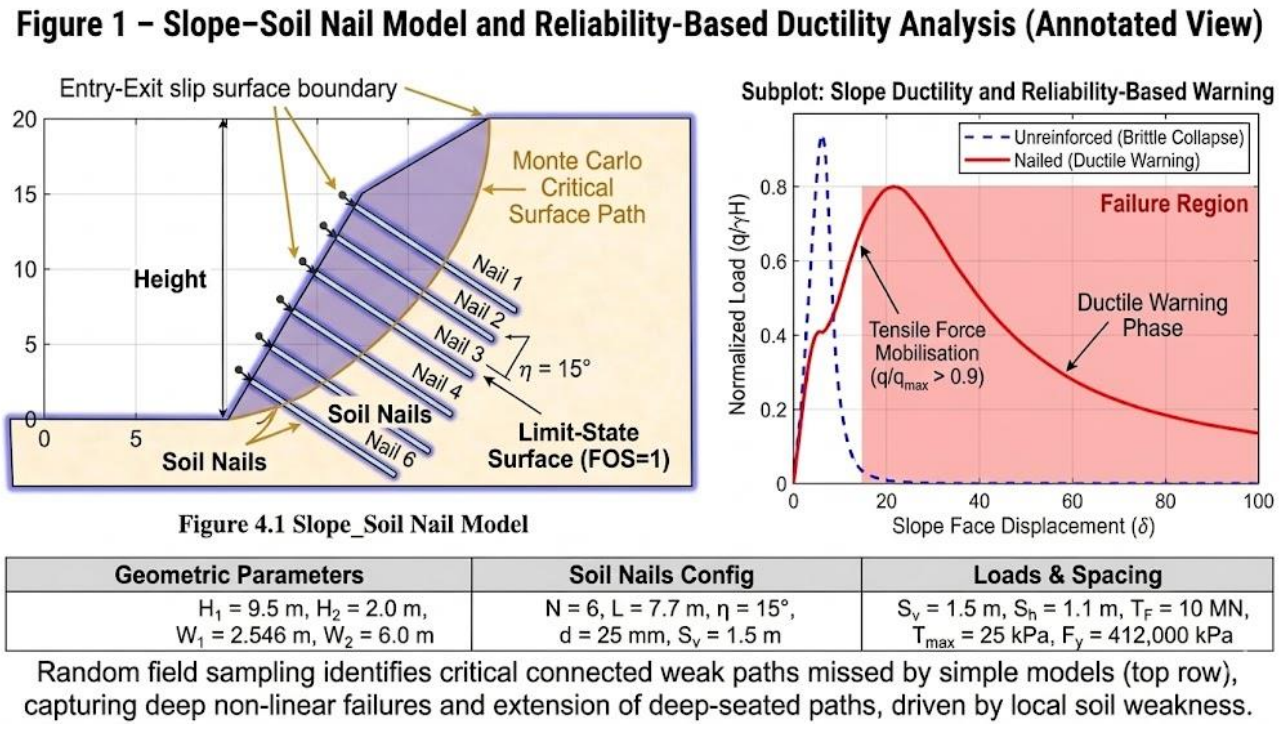

Figure 4.1 Slope_Soil Nail Model

Figure 1 – Slope–soil nail model (Figure 4.1 from source). Two-tier geometry with six soil nails inclined at 15° from horizontal. Entry–Exit slip surface boundary shown.

3. Analysis Approaches

3.1 Case 1 – FORM with Set-Varied Parameters

In Case 1 the soil is treated as homogeneous, and c' and φ' are assigned chosen scalar values that are systematically varied across five levels while the other parameter remains fixed. For each combination FORM determines the reliability index β as the shortest distance (in standardised normal space) from the origin to the limit-state surface.

The performance function g is evaluated at the mean values of the random variables, and its gradient is used to locate the design point iteratively. The probability of failure is then obtained from the standard normal CDF:

$$Pf \approx \Phi(-\beta) \quad (1)$$

The reliability index used here follows the Kulhawy–Phoon (2002) formulation:

$$\beta = \frac{ln\left[MFS \cdot \sqrt{\frac{1+CoVF^2}{1+CoVQ^2}} \right]}{\sqrt{\left[ln\left((1+CoVF^2)(1+CoVQ^2)\right) \right]}} \quad (2)$$

where MFS is the mean factor of safety; CoVF and CoVQ are the coefficients of variation of the load and resistance respectively; and σF, σQ are their standard deviations. The factor of safety for each trial slip surface is computed by the method of slices, with the circle defined by an Entry–Exit pair (Xin, Yin) → (Xout, Yout) and radius R determined by minimising FOS over the space of possible circles:

$$FOS = \Sigma \frac{\left[c' \cdot \Delta L + W_i cos\, \alpha_i \cdot tan\, \varphi' \right]}{\Sigma \left[W_i sin\, \alpha_i \right]} \quad (3)$$

where ΔL is the arc length, W_i the slice weight, and α_i the base inclination of slice i. Nail contributions enter through additional axial resistance terms projected onto the failure surface. All computations are implemented in MATLAB.

3.2 Case 2 – Monte Carlo Simulation on Random Field Realisations

In Case 2, the scalar soil parameters of Case 1 are replaced by spatially correlated Gaussian random fields. A random field $a(x, \omega)$ is fully characterised by its mean d(x), variance σ², and autocorrelation function. Following Vanmarcke (1983), the exponential autocorrelation model is used:

$$\rho(\Delta z) = exp\left(-\frac{2|\Delta z|}{\theta}\right) \quad (4)$$

where |Δz| is the separation distance and θ is the scale of fluctuation governing how rapidly the correlation decays with distance. Separate autocorrelation distances are used in the horizontal and vertical directions (anisotropic correlation), with $c_0 = [0.2, 1]$ in the MATLAB implementation.

The random fields are discretised using the Karhunen–Loève (KL) expansion, which represents the random field as a truncated series of deterministic spatial functions (eigenfunctions of the covariance operator) weighted by uncorrelated random variables:

$$a(x, \omega) = d(x) + \Sigma_{m=1}^{M} \sqrt{\lambda_m} \cdot a_m(x) \cdot \xi_m(\omega) \quad (5)$$

where λ_m and $a_m(x)$ are the eigenvalues and eigenfunctions of the integral operator C: $L^2(D) \rightarrow L^2(D)$ with covariance kernel c(x, y), and $\{\xi_m\}$ are uncorrelated zero-mean unit-variance random variables. The truncation level M is chosen such that the retained variance exceeds 95% of the total:

$$\| a - a^M \|^2 = \Sigma_{m=m+1}^{\infty} \lambda_m \rightarrow 0 \quad (6)$$

Once the random field is generated over the 2-D mesh of slice base midpoints, each element of the discretised failure surface is assigned its own spatially correlated value of cohesion and friction angle. The reliability analysis then proceeds via Monte Carlo Simulation (MCS): a large number of realisations are drawn, the factor of safety is computed for each, and the fraction of realisations with FOS < 1 estimates Pf. Adaptive Radial Based Importance Sampling (ARBIS) supplements MCS to reduce variance in the tail estimate of Pf, which is critical when failure probabilities are small.

Table 1 – **Method Comparison: Case 1 vs Case 2**

	Case 1 – FORM (Set-Varied)	**Case 2 – MCS / ARBIS (Random Fields)**
Soil model	Homogeneous; parameters set at scalar values	Spatially correlated Gaussian random fields (KL expansion)
Key inputs	Mean, variance, CoV of c′ and φ′	Autocorrelation function; scale of fluctuation θ; σ
Failure surface	Entry–Exit circular arc (FORM optimisation)	Multiple realisations; linear & non-linear surfaces captured
Spatial variability	Not represented	Explicitly modelled; each element gets unique c′, φ′
Method	FORM (first-order linearisation)	MCS + ARBIS (importance sampling)
Output	β, Pf, FOS per parameter set	β, Pf, FOS per random field realisation
Anchored/Non-anchored	Compared for each parameter combination	Compared across realisations
Computational cost	Low	Moderate to high (100+ simulations)

4. Results: Case 1 – Set-Varied Parameters (FORM)

4.1 Effect of Varied Cohesion at Fixed Friction Angle

Table 2 presents the FORM results when cohesion is varied from 5 to 25 kPa while friction angle is held constant at $\varphi' = 35°$. FOS increases monotonically with cohesion, rising from 1.333 at $c' = 5$ kPa to 1.811 at $c' = 25$ kPa (global FOS). The critical minimum FOS (FOS_1), which reflects the worst-case Entry–Exit circle, tracks this increase from 1.053 to 1.601. The reliability index β rises steeply from 3.53 to 8.69 and the probability of failure drops correspondingly by fourteen orders of magnitude, from 2.04×10^{-4} to 1.74×10^{-18}. Anchoring consistently elevates the minimum FOS: for $c' = 10$ kPa, FOS_1 jumps from 1.192 (non-anchored) to 1.953 (anchored), representing a 64% improvement.

Table 2 – Effect of Varied Cohesion with Fixed Friction Angle ($\varphi' = 35°$)

C' Cohesion (kPa)	5.0	10.0	15.0	20.0	25.0
φ' Friction Angle	35°	35°	35°	35°	35°
FOS (mean)	1.3330	1.4571	1.5751	1.6930	1.8110
FOS_1 (critical)	1.0534	1.1918	1.3301	1.4672	1.6007
β (Reliability Index)	3.5342	5.5615	6.4594	7.5165	8.6944
Pf	2.04×10^{-4}	1.34×10^{-8}	5.26×10^{-11}	2.81×10^{-14}	1.74×10^{-18}
FOS min – Non-anchored	1.0534	1.5383	1.3301	1.4672	1.6007
FOS min – Anchored	1.3526	1.9531	1.5899	1.7085	1.8271

The smooth monotonic behaviour in Table 1 is characteristic of FORM with set-varied parameters. Because the entire slope is assigned the same cohesion value, increasing that value uniformly strengthens every slice simultaneously. No pathological failure pathway can emerge.

4.2 Effect of Varied Friction Angle at Fixed Cohesion

Table 3 shows results when friction angle varies from 10° to 30° with cohesion fixed at $c' = 5$ kPa. At low friction angles the slope is unstable: FOS = 0.445 and $FOS_1 = 0.369$ at $\varphi' = 10°$. Stability improves progressively but only exceeds unity at $\varphi' = 30°$ (FOS = 1.134, non-anchored). The reliability index follows a non-monotonic pattern: β drops from 5.79 at $\varphi' = 10°$ to a minimum of 0.25 at $\varphi' = 25°$ before recovering to 1.47 at $\varphi' = 30°$. This inversion reflects the interaction between the orientation of soil particles and the critical failure geometry near the threshold of instability, where small parameter changes cause large shifts in Pf.

Table 3– Effect of Fixed Cohesion (c′ = 5 kPa) with Varied Friction Angle					
C' Cohesion (kPa)	5.0	5.0	5.0	5.0	5.0
φ' Friction Angle	10°	15°	20°	25°	30°
FOS (mean)	0.4446	0.6128	0.7785	0.9536	1.1340
FOS_i (critical)	0.3685	0.4887	0.6142	0.7748	0.8929
β (Reliability Index)	5.7908	4.3322	2.5208	0.2521	1.4685
Pf	3.50×10^{-9}	7.38×10^{-6}	0.0059	0.3002	0.0710
FOS min – Non-anchored	0.3685	0.4887	0.6142	0.7480	0.8929
FOS min – Anchored	0.4617	0.6171	0.7802	0.9542	1.1433

Notably, at φ′ = 25° the probability of failure is 0.30 meaning there is a 30% chance of failure despite a global FOS of 0.954. This underscores the importance of the reliability index as a more discriminating metric than FOS alone. The anchored slope shows improved minimum FOS across all friction angle levels.

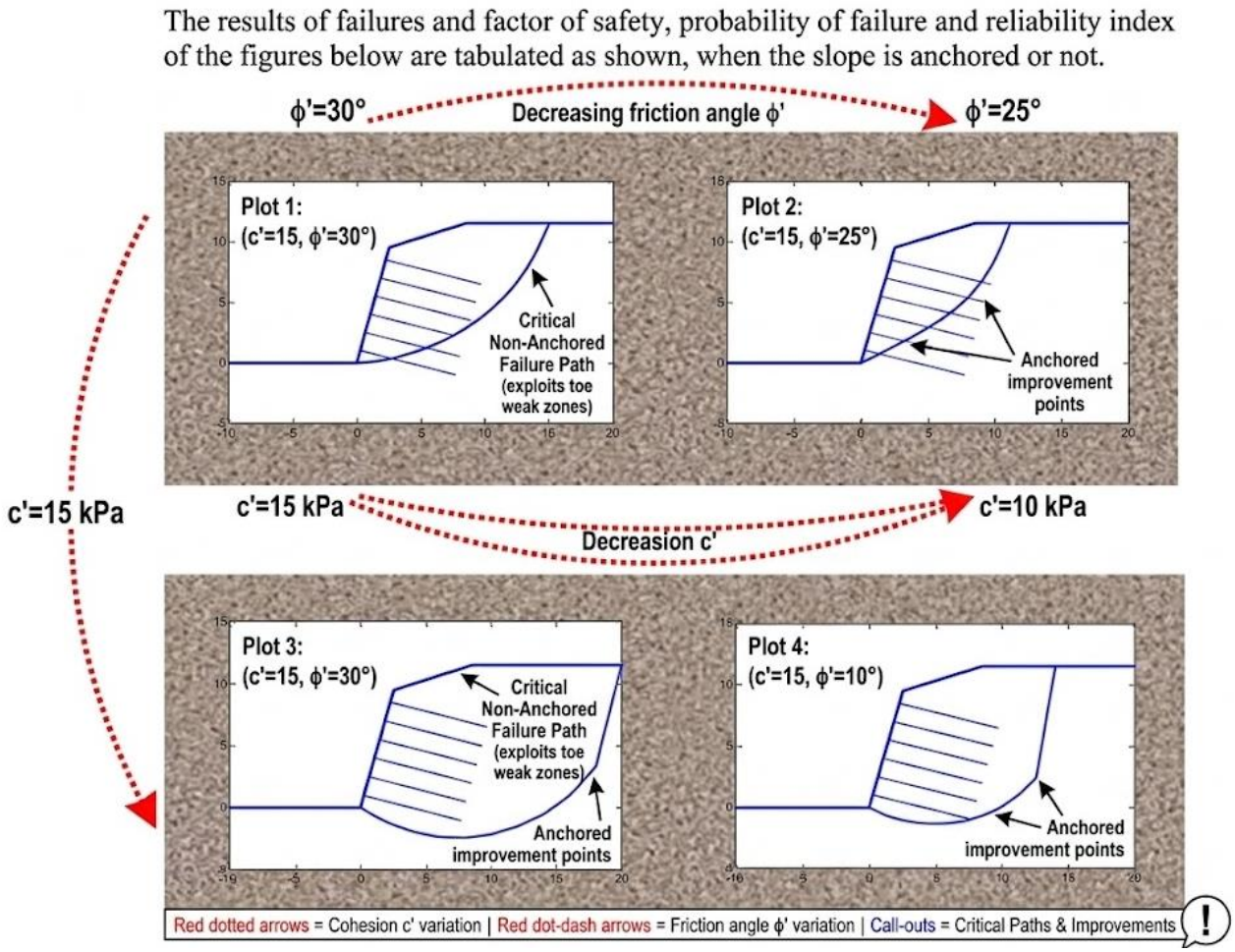

Figure 3 – Modes of failure for non-random fields (Case 1): Four slip surface configurations under varied cohesion and friction angle. Trial surfaces modelled with Entry–Exit method; all exit at the slope toe. Homogeneous soil assumed.

5. Results: Case 2 – Random Field Realisations (MCS / ARBIS)

5.1 Random Field Generation and Characterisation

Five independent random field realisations were generated for each of cohesion and friction angle using the correlated Gaussian random field generator in MATLAB, employing the KL expansion (Equation 5) truncated at M = 10 terms. The 2-D mesh was constructed over the slope domain with an exponential autocorrelation structure. Two mesh resolutions were tested: 50 × 50 and 150 × 150, with the finer mesh producing more localised and spatially detailed variability patterns.

In each realisation, the mean cohesion is $\bar{c}' = 5$ kPa with CoV = 0.10 ($\sigma = 0.5$ kPa), and the mean friction angle is $\bar{\varphi}' = 35°$ with CoV = 0.10 ($\sigma = 3.5°$). These parameters are consistent with the scalar inputs of Case 1, enabling a direct comparison. The random fields exhibit spatially correlated patches of above- and below-average strength some realisations have large contiguous weak zones that can span a significant portion of a potential failure surface.

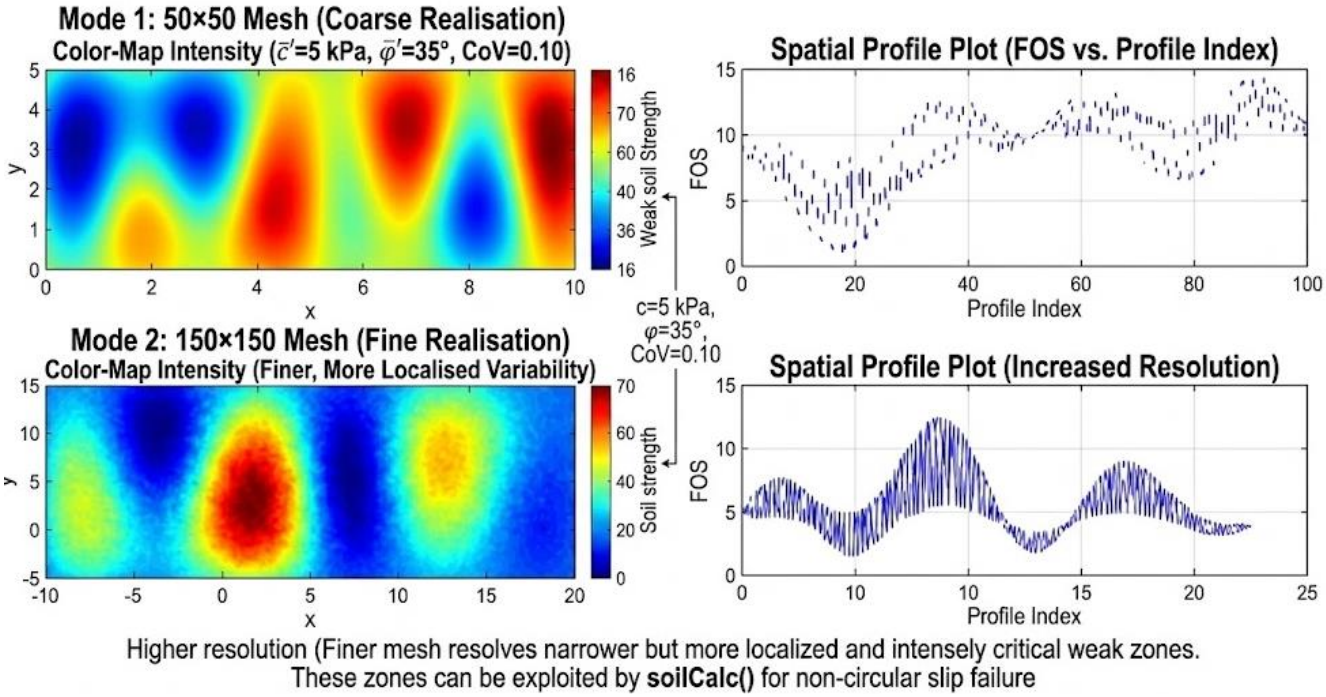

Figure 4 – Generated random fields (MATLAB). Left: colour-map of field intensity (blue = low, red = high). Right: spatial profile plot. Top row: 50×50 mesh; Bottom row: 150×150 mesh showing finer, more localised variability.

5.2 Failure Modes and Reliability Outputs

Table 3 presents the reliability results across five random field realisations. Several features distinguish these results sharply from the Case 1 outputs. First, the global FOS values vary widely (1.47 to 4.69), reflecting the stochastic nature of the input fields a realisation with predominantly strong soil returns a high mean FOS, while one with a

weak zone near the critical surface returns a lower value. Second, and more critically, the minimum (critical) FOS values are substantially lower than the global FOS in every realisation, ranging from 0.562 to 1.097. This divergence between global and critical FOS has no analogue in Case 1.

Third, the probabilities of failure are non-negligible across all five realisations (Pf ranges from 0.071 to 0.456), despite global FOS values well above unity. This is the central finding: the presence of spatially localised weak zones invisible to FORM creates failure pathways that are consistent with the statistical distribution of soil strength yet would be completely missed by a scalar parameter analysis.

Fourth, the failure surfaces identified by Case 2 include both linear (planar) and non-linear (irregular) geometries. FORM's circular arc approximation cannot replicate the non-linear surfaces; this is the mathematical consequence of its linearisation assumption at the design point.

Table 3 – Effect of Random Fields: Cohesion and Friction Angle (MCS / ARBIS)					
C' Cohesion	Random C′	Random C′	Random C′	Random C′	Random C′
φ' Friction Angle	Random φ′	Random φ′	Random φ′	Random φ′	Random φ′
FOS (global)	1.8933	4.6945	2.6795	3.8984	1.4726
FOS$_i$ (critical)	1.0974	0.9377	0.8598	0.7716	0.5621
β (Reliability Index)	0.1150	0.6293	1.4221	1.4714	1.3205
Pf	0.4556	0.2646	0.0775	0.0706	0.0933
FOS min – Non-anchored	0.9698	0.7693	0.6494	0.6865	0.8314
FOS min – Anchored	1.2656	1.1825	0.8684	1.1454	1.0111

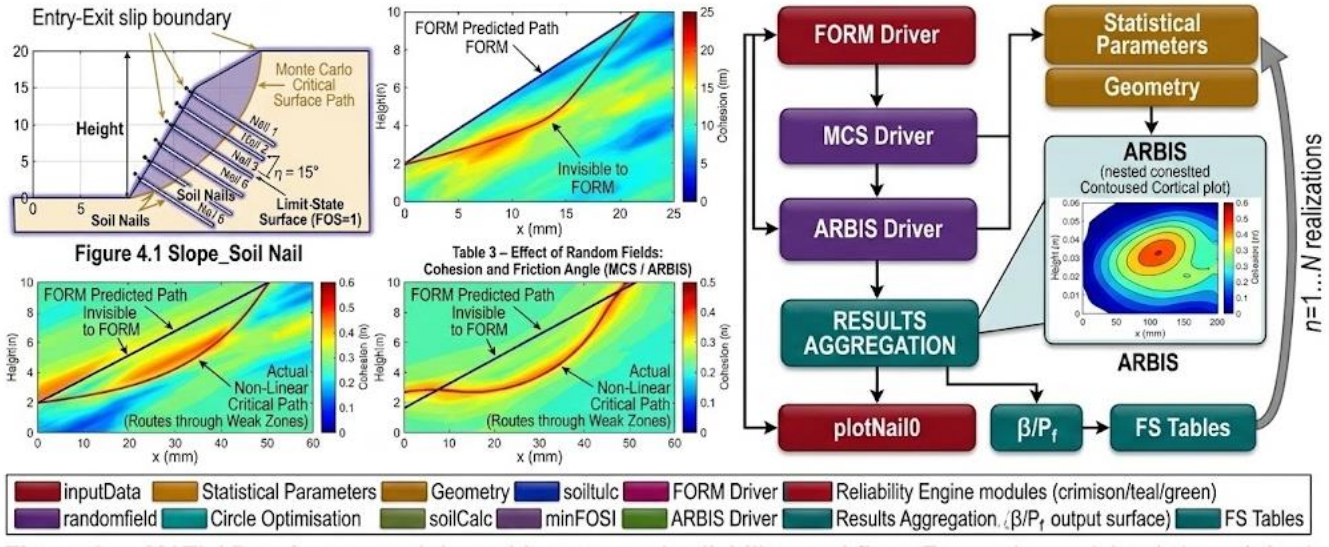

Figure 5 – Modes of failure for random fields (Case 2): Four realisations with random cohesion and friction angle. Failure surfaces are both linear and non-linear. Background texture reflects the spatially variable soil realisation.

6. Comparative Discussion

6.1 Factor of Safety

Case 1 yields a single, deterministic FOS for each parameter combination. The FOS is sensitive to changes in c′ or φ′ but responds symmetrically and monotonically. Case 2 reveals that the mean global FOS can be misleadingly high: Realisation 2 has a global FOS of 4.69 yet a critical FOS of only 0.94, implying the slope is technically unstable along its most dangerous slip surface. This disconnect arises because the weak zone in Realisation 2 is spatially isolated and does not dominate the global equilibrium, but it is precisely located along the critical failure path.

6.2 Reliability Index and Probability of Failure

The reliability indices in Case 1 span a wide range (3.5 to 8.7 for the cohesion sweep) and are firmly in the 'good' to 'high' category on standard performance scales. The corresponding failure probabilities are negligibly small. In Case 2, the reliability indices cluster between 0.12 and 1.47, corresponding to Pf values between 7% and 46%. According to the same performance classification, these correspond to 'hazardous' to 'below average' performance levels a fundamentally different conclusion for a slope with ostensibly the same mean soil properties.

The discrepancy is not a computational artefact; it is a physical consequence of heterogeneity. When spatial variability is properly represented, the probability of encountering a weak-zone-dominated failure path in a random sample of 'equivalent' soil masses is substantially higher than FORM predicts.

6.3 Anchored vs. Non-Anchored Performance

Both approaches agree that anchoring (soil nailing) consistently improves the minimum FOS. In Case 1, the improvement ranges from approximately 7% to 64% depending on the parameter combination. In Case 2, the improvement is similarly consistent: every realisation shows a higher anchored FOS, and three of five realisations achieve FOS > 1.0 only when anchored. This convergence between the two approaches on the qualitative benefit of nailing provides confidence that the soil nail design is robust to the method of analysis.

The quantitative difference is more important: the random field approach identifies realisations (e.g., Realisation 3) where even the anchored slope barely achieves FOS > 1 (FOS_anchored = 0.868), suggesting that for some physically plausible spatial distributions of soil strength, the nail configuration is insufficient. No such finding emerges from Case 1, where FOS always exceeds 1.0 for comparable mean values.

6.4 Mean FOS > 1 Does Not Guarantee Safety

Perhaps the most practically significant result is the demonstration that a mean FOS > 1 is consistent with Pf values up to 46%. This occurs because the factor of safety is a nonlinear function of the spatially distributed soil strength: failure is controlled by the weakest path through the soil, not the average strength. Duncan (2000) warned that applying a uniform factor of safety to conditions with varying degrees of uncertainty is logically inconsistent. The random field results quantify exactly the magnitude of this inconsistency.

The variance reduction function introduced by Vanmarcke (1983) explains this quantitatively: the effective variance of the average soil strength over a potential failure surface depends on the ratio of the surface length to the scale of fluctuation. When the scale of fluctuation is comparable to or larger than the failure surface length, spatial averaging provides little variance reduction, and the effective soil variability seen by the failure mechanism is close to the point-level variability. This is the regime that characterises the realisations in Table 3.

Code Snippet 1 – Random Field Assignment in soilCalc () (MATLAB)

The following excerpt from the soilCalc () subroutine illustrates how random field values are mapped to individual slice elements before the factor of safety summation. This is the critical line of differentiation between Case 1 (scalar c, φ) and Case 2 (spatial arrays Coh(i), Phi(i)):

```
%  Build correlation structure (exponential, anisotropic)
corr.name = 'exp';
corr.c0   = [1 1];          % anisotropic correlation lengths
corr.sigma = 0.5;  mean_c = 5;

%  Generate random field of cohesion over the slice-base mesh
[Coh, KL] = randomfield(corr, mesh, 'mean', mean_c, 'trunc', 10);
mean_phi   = pi * 35 / 180;
corr.sigma = 0.1 * mean_phi;
%  Generate random field of friction angle
[Phi, KL] = randomfield(corr, mesh, 'mean', mean_phi, 'trunc', 10);
%  Factor-of-safety summation with spatially varying c and phi
for i = 1 : N
   QQ = QQ + (Coh(i) * Arc(i)) + Weight(i) * cos(Alpa(i)) * tan(Phi(i));
   LL = LL + Weight(i) * sin(Alpa(i));
end
%  FOS = QQ / LL  (computed in caller)
```

In Case 1 the line inside the loop reads QQ = QQ + (Coh*Arc(i)) + ..., where Coh is a scalar. Replacing that scalar with the spatially indexed array Coh(i) is the sole but consequential modification that transitions the analysis from Case 1 to Case 2.

7. Conclusions

This paper has compared deterministic parameter variation via FORM (Case 1) with random field Monte Carlo / ARBIS analysis (Case 2) for a soil-nailed slope. The following conclusions are drawn:

1. FORM with set-varied parameters produces smooth, monotonically improving reliability metrics as mean soil strength increases. It correctly identifies the beneficial effect of soil nailing but cannot detect localised failure modes arising from spatial heterogeneity.
2. Random field analysis reveals that the mean factor of safety can significantly overestimate structural reliability. In all five realisations studied, Pf ranged from 7% to 46% despite global FOS values between 1.47 and 4.69. This is due to spatially localised weak zones that create credible failure paths invisible to scalar-parameter FORM.
3. Critical (minimum) FOS values from Case 2 are consistently lower than global FOS values, and in several realisations the slope is formally unstable ($FOS_l < 1$) without anchoring. Case 1 does not reproduce this finding for equivalent mean parameters.
4. Both approaches agree on the qualitative benefit of soil nailing: anchoring improves the minimum FOS in every realisation. The random field approach additionally identifies edge cases where nailing is insufficient, informing more conservative design decisions.
5. The Karhunen–Loève expansion implemented via the MATLAB randomfield() function provides an efficient and flexible mechanism for generating spatially correlated soil fields. Truncating at M = 10 terms retains sufficient variance for the autocorrelation lengths considered here.
6. Future work should incorporate groundwater level variability, seepage forces, and dynamic (seismic) loading into the random field framework. The effect of nail diameter and nail spacing on random-field-predicted failure probability also warrants systematic investigation.

References

[1] Vanmarcke, E. H. (1983). Random Fields – Analysis and Synthesis. MIT Press, Cambridge, MA.

[2] Baecher, G. B. and Christian, J. T. (2003). Reliability and Statistics in Geotechnical Engineering. John Wiley & Sons, Chichester.

[3] Cornell, C. A. (1969). A probability-based structural code. Journal of the American Concrete Institute, 66(12), 974–985.

[4] Kulhawy, F. H. and Phoon, K. K. (2002). Observations on geotechnical reliability-based design development in North America. Proc. Int. Workshop on Foundation Design Codes, Kamakura, 31–48.

[5] Griffiths, D. V. and Fenton, G. A. (2009). Probabilistic settlement analysis by stochastic and random finite element methods. Journal of Geotechnical and Geoenvironmental Engineering, 135(11), 1629–1637.

[6] Duncan, J. M. (2000). Factor of safety and reliability in geotechnical engineering. Journal of Geotechnical and Geoenvironmental Engineering, 126(4), 307–316.

[7] Phoon, K. K. and Kulhawy, F. H. (1999). Characterisation of geotechnical variability. Canadian Geotechnical Journal, 36, 612–624.

[8] El-Ramly, H., Morgenstern, N. R. and Cruden, D. M. (2002). Probabilistic slope stability analysis for practice. Canadian Geotechnical Journal, 39, 665–683.

[9] Sudret, B. and Der Kiureghian, A. (2002). Comparison of finite element reliability methods. Probabilistic Engineering Mechanics, 17, 337–348.

[10] Enevoldsen, I. and Sørensen, J. D. (1994). Reliability-based optimization in structural engineering. Structural Safety, 15(3), 169–196.

[11] Elkateb, T., Chalaturnyk, R. and Robertson, P. K. (2002). An overview of soil heterogeneity: quantification and implications on geotechnical field problems. Canadian Geotechnical Journal, 40, 1–15.

[12] Luo, Z., Atamturktur, S., Juang, C. H., Huang, H. and Lin, P. S. (2011). Probability of serviceability failure in a braced excavation in spatially random field: Fuzzy finite element approach. Computers and Geotechnics, 38, 1031–1040.

[13] Schweiger, H. F. and Peschl, G. M. (2005). Reliability analysis in geotechnics with the random set finite element method. Computers and Geotechnics, 32(6), 422–435.

[14] Rackwitz, R. (2000). Reviewing probabilistic soils modelling. Computers and Geotechnics, 26, 199–223.

[15] Taib, S. N. L. (2010). A review of soil nailing approaches. UNIMAS E-Journal of Civil Engineering, 1(2).

[16] Honjo, Y. (2011). Challenges in geotechnical reliability based design. ISGSR 2011, Bundesanstalt für Wasserbau, ISBN 978-3-939230-01-4.

[17] Mohsen, A., Kourosh, S., Mostafa, S. and Mehrdad, H. (2011). Uncertainty and reliability analysis applied to slope stability: a case study from Sungun Copper Mine. Geotechnical and Geological Engineering, 29, 581–596.

[18] US Army Corps of Engineers (1995). Introduction to Probability and Reliability Methods for Use in Geotechnical Engineering. ETL 1110-2-547.